(11) Rinaudo, M. In *Polyelectrolytes*; Sêlègny, E., Ed.; Reidel: Dordrecht, Holland, 1974; p 157.
(12) Manning, G. S. In ref 11, p 9.
(13) Kwak, J. C. T.; O'Brien, M. C.; MacLean, D. A. *J. Phys. Chem.* **1975**, *79*, 2381.
(14) Hayakawa, K.; Kwak, J. C. T. *J. Phys. Chem.* **1983**, *87*, 506.
(15) Kwak, J. C. T. *J. Phys. Chem.* **1973**, *77*, 2790.
(16) Kohn, R. *Pure Appl. Chem.* **1975**, *42*(3), 371.
(17) Kohn, R.; Luknar, O. *Collect. Czech. Chem. Commun.* **1975**, *40*, 1959.
(18) Rees, D. A. *Chem. Ind. (London)* **1972**, 630.
(19) Grant, G. T.; Morris, E. R.; Rees, D. A.; Smith, P.J. C.; Thom, D. *FEBS Lett.* **1973**, *32*, 195.
(20) Podlas, T. J.; Ander, P. *Macromolecules* **1970**, *3*, 154.
(21) Ise, N.; Okubo, T. *Macromolecules* **1978**, *11*, 439.
(22) Tondre, C.; Zana, R. *J. Phys. Chem.* **1971**, *75*, 3367.
(23) Rinaudo, M.; Milas, M. In *Polyelectrolytes and Their Applications*; Sêlègny, E., Ed.; Reidel: Dordrecht, Holland, 1975; p 31.
(24) Lawton, J. B.; Phillips, G. O. *Text. Res. J.* **1975**, *45*, 5.
(25) Karenzi, P. C.; Meurer, B.; Spegt, P.; Weill, G. *Biophys. Chem.* **1979**, *9*, 181.
(26) Strauss, U. P.; Leung, Y. P. *J. Am. Chem. Soc.* **1965**, *87*, 1476.
(27) Eldridge, R. J.; Treloar, F. E. *J. Phys. Chem.* **1970**, *74*, 1446.
(28) Westra, S. W. T.; Leyte, J. C. *J. Magn. Reson.* **1979**, *34*, 475.
(29) Koda, S.; Nomura, H.; Nagasawa, M. *Biophys. Chem.* **1983**, *18*, 361.
(30) Manning, G. S. *J. Phys. Chem.* **1984**, *88*, 6654.

Deuteration Effects on the Miscibility and Phase Separation Kinetics of Polymer Blends

Hsinjin Yang,† Mitsuhiro Shibayama,‡ and Richard S. Stein*

Polymer Research Institute, University of Massachusetts, Amherst, Massachusetts 01003

Nobuyuki Shimizu and Takeji Hashimoto

Department of Polymer Chemistry, Kyoto University, Kyoto 606, Japan.
Received October 28, 1985

ABSTRACT: The substitution of deutereous polystyrene (PSD) for hydrogenous PS (PSH) in PS/poly(vinyl methyl ether) (PVME) blends raised the lower critical solution temperature (LCST) of the blend by about 40 °C. This deuteration effect has been qualitatively interpreted as resulting partially from the larger percentage of negative excess volume of mixing for PSD/PVME relative to that of PSH/PVME. Both blends have the same glass transition temperature (T_g) for the same composition. Optical microscopy was used to study the morphology of phase separation for PSD/PVME and PSH/PVME blends at the same degree of superheating. The composition for these blends is close to the critical composition, i.e., 30 wt % PS. The observed morphologies are consistent with the prediction of the Cahn–Hilliard theory for spinodal decomposition. It has been found that the kinetics of phase separation for the PSD blend is about 10 times faster than that for the PSH blend. This behavior can be qualitatively interpreted in terms of the William–Landel–Ferry (WLF) equation. Furthermore, dynamic parameters, maximum scattering vector magnitude (q_m) and time (t) of spinodal decomposition for the above blends studied by light scattering are scaled to the reduced wave number and time, Q_m and τ, respectively, in terms of the characteristic parameters—apparent diffusion constant (D_{app}) and $q_m(t=0)$. The phase separation process is found to be the same for PSD/PVME, PSH/PVME, and other systems such as metallic alloys, inorganic glasses, and small-molecule systems. Their exponent has the same value (1.0) according to the power-law approach. The difference in the phase separation kinetics between the PSD/PVME and the PSH/PVME blends is simply due to lower viscosity and higher diffusion constant for the PSD blend.

Introduction

The small-angle neutron scattering (SANS) technique has often been used to study the miscibility of polymer blends in the solid state by using the deuterium substitution technique.[1-10] The substitution of deuterium for hydrogen in one of the components of the polymer blend provides the difference in a scattering length necessary to obtain sufficient coherent scattering. In this type of substitution, it is usually assumed that the thermodynamic interaction between components is negligibly affected. That is, for hydrogenous (H) and deutereous (D) species of one component and a second component (S) the Flory interaction parameters χ_{HS} and χ_{DS} are assumed to be equal and χ_{HD} is assumed to be zero. The validity of the latter assumption in the case of hydrogenous and deutereous polystyrene (PSH and PSD) has been demonstrated through the observation of a zero second virial coefficient by SANS studies from Zimm plots.[11] It should be pointed out that a small difference in thermodynamic properties between PSH and PSD has been demonstrated[12] by studies on solutions of both polymers in hydrogenous and deutereous cyclohexane. A lower critical solution temperature (LCST) behavior[13] is seen for a blend of polystyrene (PS) and poly(vinyl methyl ether) (PVME); its value depends on the molecular weight of the components.[14] In our previous paper,[15] we have shown by using photometric light scattering that the substitution PSD for PSH in PS/PVME blends raised the LCST by about 40 °C. This phenomenon has also been verified by Halary et al. using the fluorescence technique.[16]

In this paper we further describe the comparison between PSD/PVME and PSH/PVME blends, considering their glass transition behavior, volume of mixing change, and phase separation behavior and its kinetics.

Experimental Section

Sample Preparation. A commercial sample of PVME (Scientific Polymer Products, Webster, NY, M_n = 46 500, M_w = 99 000, and M_w/M_n = 2.13) was solution blended with samples of anionically synthesized hydrogenous polystyrene (M_w = 100 000, M_w/M_n = 1.05) or with deutereous polystyrene (M_w = 119 000,

† Part of his Ph.D. Dissertation.
‡ Current address: Department of Polymer Science and Engineering, Kyoto Institute of Technology, Kyoto 606, Japan.

0024-9297/86/2219-1667$01.50/0

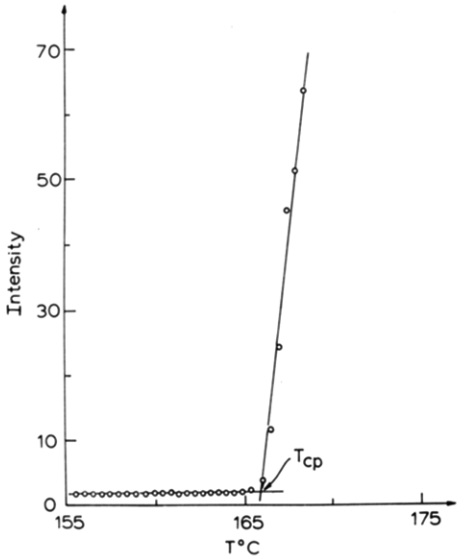

Figure 1. Cloud point determination for 20/80 wt % PSD/PVME.

M_w/M_n = 1.05) (Polymer Laboratories, Stove, OH). Prior to blending the PVME was dried at 60 °C under vacuum for at least 1 day, at which time constant weight was reached. Films of PSH (or PSD)/PVME mixtures were cast from 10% toluene solutions at room temperature on the glass slides. All films were dried in an oven under nitrogen at room temperature for 1 day followed by 3 days at 70 °C under nitrogen in order to remove all the solvent and then slowly cooled down to the ambient temperature. The thickness of the films was about 10–15 μm. It is noted that these films are considerably thicker than those utilized by Reich and Cohen,[17] where a dependence of transition behavior on thickness was observed.

Differential Scanning Calorimetry (DSC) Measurements. The most commonly used method for establishing miscibility in polymer blends or partial phase mixing in such blends is from studies of their glass transition temperature (T_g). The thermal transition in polymer samples and blends were investigated by using a Perkin-Elmer Model DSC-2. The weight of each sample was typically 12–20 mg; a heating rate of 20 °C/min and a range of 3 mcal/s were employed. The DSC scans were used to establish the T_g from an observation of the onset of the transition.

Light Cloud Point Measurements. Light cloud points were obtained by measuring the intensity of light at an angle of 20° with a photometric light scattering apparatus. Samples were heated at a rate of 2 °C/min, and intensities were recorded as a function of temperature. Phase separation was characterized by an upturn in scattered intensity as the temperature was increased, as shown in Figure 1. The intersection of straight lines drawn through portions of the curve below and above the break was taken as the transition temperature.

Density Measurements. The densities of the films of PSD/PVME, PSH/PVME, and a ternary mixture of PSD/PSH/PVME were measured in a density gradient column at 25 °C. While most of the data is for samples above their T_g, the sample having the highest PS content had T_g above room temperature; consequently, its density may be affected by excess free volume resulting from solvent casting and annealing to form a film at a temperature below T_g.

Optical Microscopy. The samples, which had a composition close to critical [30/70 wt % of PSD (M_w = 119000)/PVME, PSH (M_w = 100000)/PVME films], were heated at the desired separation temperature for different periods of time and then quenched with liquid nitrogen to freeze the structure at that specific condition. The treated samples were examined by optical microscopy with a high magnification lens at room temperature to observe the phase separation behavior.

Light Scattering Studies. Light scattering was used to study blends of PSH/PVME and PSD/PVME at the critical composition. They were heated such that the degree of superheating ($\Delta T = T - T_s$, where T_s is the spinodal temperature) was the same in both cases. The blends were placed on a Mettler hot stage, which had been preheated to the desired experimental temperature, and the light scattering profile was recorded during the process of phase separation. The data were collected simultaneously over an entire angular range (2θ).

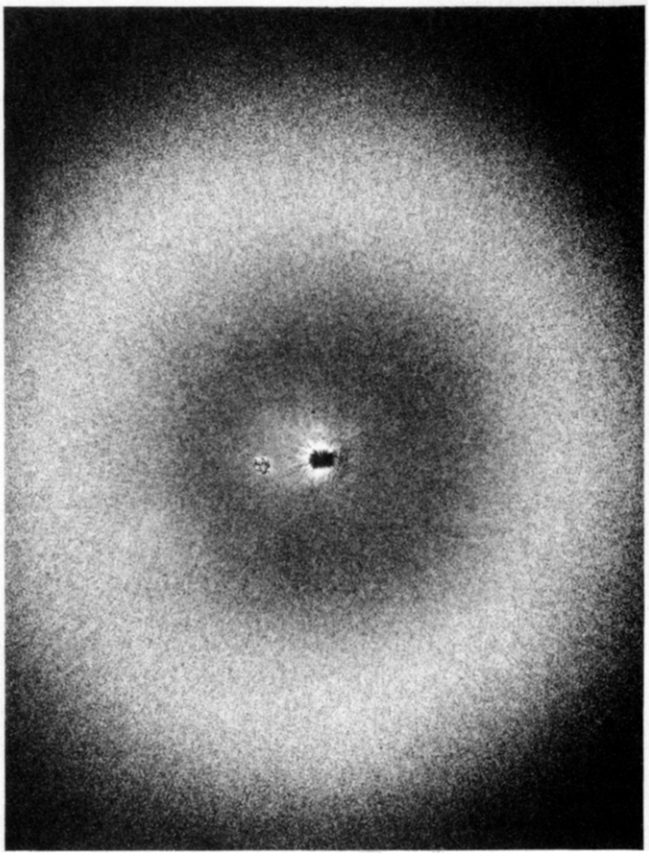

Figure 2. Observed light scattering pattern resulting from phase separation in polymer blends.

The early stages of phase separation were studied by wide-angle light scattering (WALS)[18] and the late stages studied by using an Optical Multichannel Analyzer-2 (OMA2), which is a device for the rapid detection of intensity in two-dimensional small-angle light scattering (SALS) patterns.[19] The typical scattering pattern for the late stages of phase separation in the unstable region from these blends is a isotropic ring shape as shown in Figure 2. The ring diameter decreases with time, indicating growth in phase size. These data are then circularly averaged and analyzed.

Results and Discussion

Cloud Points. Phase diagrams were characterized by using optical cloud points. It should be noted that cloud points can be affected by heating rate as shown in Figure 3 as a consequence of kinetics of phase separation. Also the cloud point strongly depends upon the molecular weight distribution. Therefore, the cloud point here is not the same as the binodal point, which should be measured under an infinitesimal heating rate and with monodisperse polymers.[20] We found a single cloud point for a blend of PVME with a mixture of PSH and PSD at a temperature intermediate between that found by using pure PSD or PSH as shown in Figure 4. The resulting cloud point curves for PSD/PVME, PSD/PSH/PVME, and PSH/PVME blends are shown in Figure 5.

Behavior of the Glass Transition Temperature (T_g). A single T_g of PSH/PVME clear films cast from toluene determined from DSC measurements has been studied by Bank et al.[21] and verified here. PSD/PVME films were observed to be clear when cast from toluene and exhibit a single T_g with varied composition, as shown in Figure 6. The glass transition temperatures obtained for PSD (M_w = 119000)/PVME and PSH (M_w = 100000)/

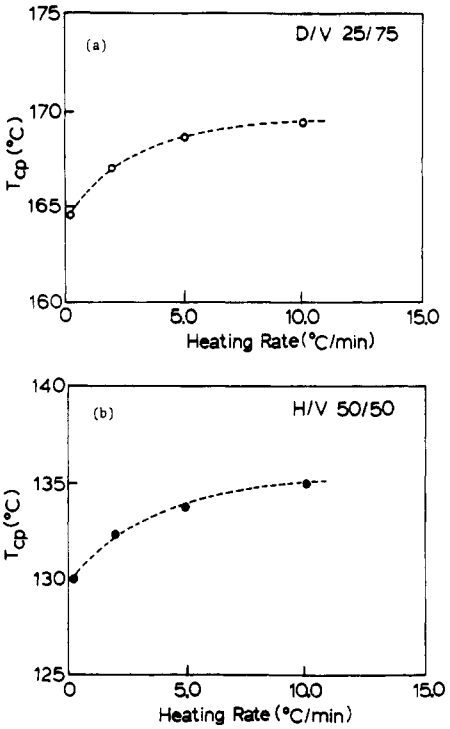

Figure 3. Cloud point (T_{cp}) vs. heating rates for (a) 25/75 wt % PSD/PVME, and (b) 50/50 wt % PSH/PVME.

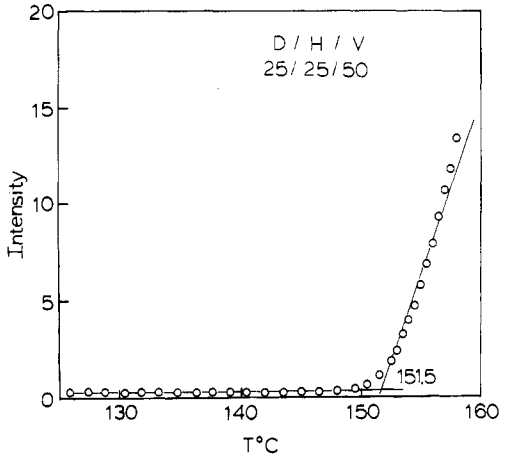

Figure 4. Cloud point determination for ternary blends PSD/PSH/PVME (25/25/50 wt %).

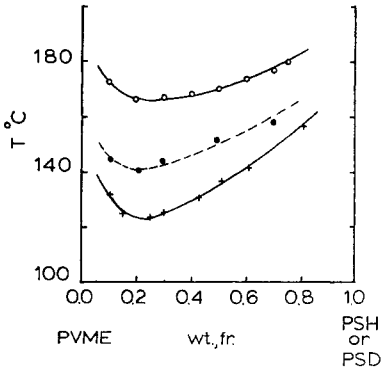

Figure 5. Cloud point curves for (○) PSD/PVME; (●) PSD/PSH/PVME; (+) PSH/PVME. PSD, M_w = 119 000, M_w/M_n = 1.05 PSH, M_w = 100 000, M_w/M_n = 1.05 PVME, M_w = 99 000, M_w/M_n = 2.13.

PVME are listed in Table I. It is seen that both systems show a single T_g that is the same for the same composition. This observation indicates that the substitution of H by D has little effect on intermolecular interaction and consequently has little influence on T_g behavior. Phase miscibility is much more sensitive to interaction differences than to T_g.

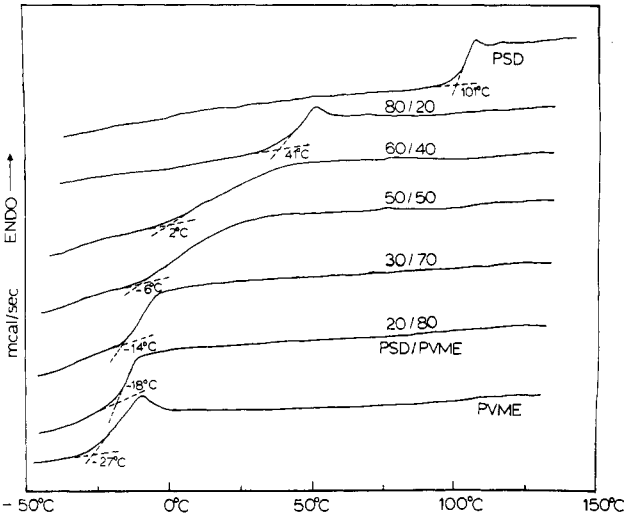

Figure 6. DSC curves for PSD/PVME blends with various compositions.

Table I
Glass Transition Temperature (T, °C) for Various Compositions of PSD/PVME and PSH/PVME Blends

blends (wt % PVVE)	PSD/PVME	PSH/PVME
100	-27	-27
80	-18	-17
70	-14	-14
50	-6	-7
40	2	3
20	41	43
0	101	101

Excess Volume of Mixing. The densities of immiscible polymer blends and phase-separated block copolymers are generally found[22,23] to agree with the values calculated from the simple additivity relationship given by[24,25]

$$1/\rho_{blend} = W_A/\rho_A + W_B/\rho_B \quad (1)$$

$$V_{blend} = W_A V_A + W_B V_B \quad (2)$$

Kwei et al. have shown that there is a negative volume change on mixing (ΔV_m) for the miscible blends of PSH/PVME,[26] with ΔV_m defined as

$$\Delta V_m = V_s - V_{blend} \quad (3)$$

where V_s is the experimental specific volume of the blend and V_{blend} is that calculated according to eq 2.

The increase in density or negative volume of mixing has been observed for PSD/PVME, PSH/PVME, and PSD/PSH/PVME systems, as shown in Table II and Figure 7. It is noted that densities were measured at room temperature, which is below T_g for the blends that are richer in PS. Consequently, for those below T_g, there may be a contribution to the specific volume associated with the excess volume in cooling through T_g. The negative volume of mixing suggests that the existence of intermolecular interactions favor better packing between molecules for all the above blends. From Table II, it is seen that PSD/PVME blends exhibit a greater negative volume change of mixing than PSH/PVME blends for all compositions. The relative percentage of negative volume of mixing ($\Delta V_m/V_{blend}$) for PSD/PVME is much larger than that for PSH/PVME, as can be seen in Figure 8. This indicates that the blend with PSD packs more densely than

Table II
Data of Measured Density for Blend Components and PSD/PVME, PSH/PVME and PSD/PSH/PVME Blends

polymer	ρ_{exptl}	V_s
PSH	1.044	0.958
PSD	1.116	0.896
PVME	1.047	0.955

wt % blend	ρ_{exptl}	V_s	V_b	ΔV_m, cm^3/g	$\Delta V_m/V_b$, %
			PSH/PVME		
10/90	1.049	0.953	0.955	−0.002	−0.209
30/70	1.058	0.945	0.955	−0.010	−1.047
50/50	1.061	0.943	0.956	−0.013	−1.360
70/30	1.060	0.943	0.957	−0.014	−1.463
90/10	1.051	0.951	0.958	−0.007	−0.731
			PSD/PVME		
10/90	1.061	0.942	0.949	−0.007	−0.738
30/70	1.079	0.927	0.937	−0.010	−1.067
50/50	1.099	0.910	0.926	−0.016	−1.723
70/30	1.112	0.899	0.914	−0.015	−1.641
90/10	1.118	0.894	0.902	−0.008	−0.887
			PSH/PSD/PVME		
15/15/70	1.068	0.937	0.946	−0.011	−1.162
25/25/50	1.079	0.927	0.941	−0.014	−1.488
35/35/30	1.087	0.920	0.935	−0.015	−1.604

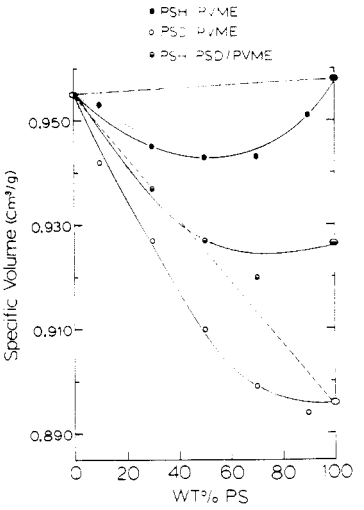

Figure 7. Volume of mixing as a function of PS concentration for PSD/PVME, PSD/PSH/PVME, and PSH/PVME blends at 25 °C.

the hydrogenous one, indicating a stronger intermolecular attraction, which is consistent with their LCST behavior. The volume changes on mixing for PSD/PSH/PVME are intermediate between those for PSH/PVME and PSD/PVME. These observations imply that the total χ parameter (χ_{net}) has two contributions, as shown in Figure 9: (1) The PSD blends have less free volume than those of PSH (greater negative volume change). This factor contributes to the increase in free energy of mixing because of the smaller entropy associated with this smaller free volume. Thus, the contribution to the χ parameter associated with this free volume reduction (χ_{vol}) increases. (2) The deuterium replacement may affect the contact energy of mixture ($\chi_{contact}$). If there is an attractive potential between PS and PVME, then a more negative volume change of mixing as found with PSD should result in these species being closer together, leading to a free energy of mixing decrease and a negative contribution to χ. Thus the increase in the LCST resulting from replacement of PSH by PSD appears to be a consequence of the latter physical factor outweighing the former one. To verify this proposal, it would be desirable to study the volume as

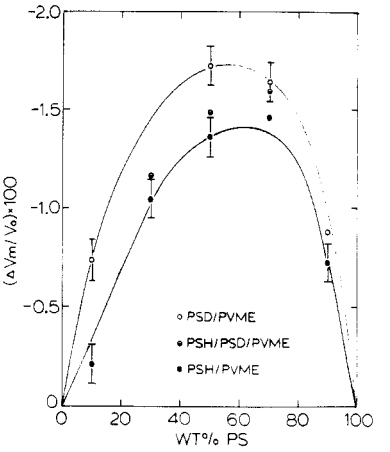

Figure 8. Comparison plot for the relative percentage of the volume of mixing change as a function of PS composition for PSD/PVME, PSD/PSH/PVME, and PSH/PVME blends at 25 °C.

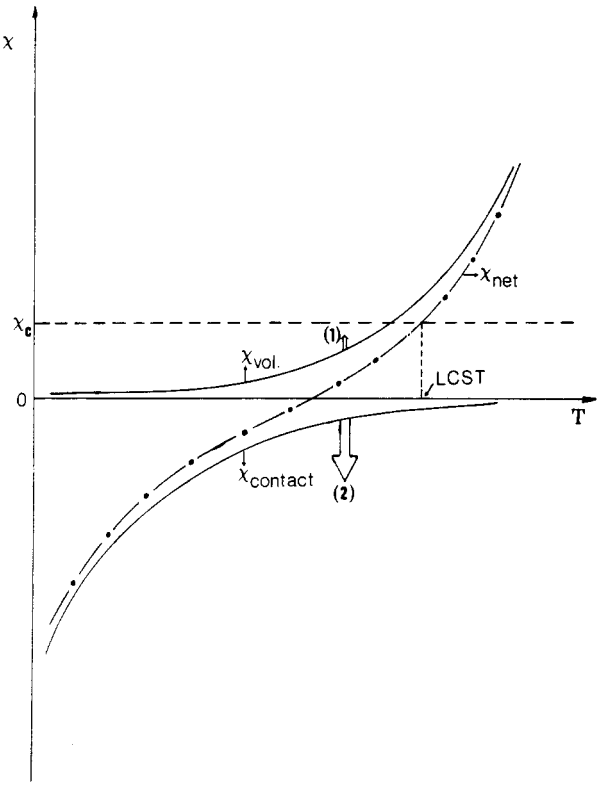

Figure 9. χ as a function of temperature for PS/PVME blends. There are two contributions to the total χ (χ_{net}): (1) χ_{vol} due to free volume; (2) $\chi_{contact}$ due to the contact energy. The second factor may outweigh the first factor due to deuteration leading to an increase of LCST of PSD/PVME.

function of temperature and/or pressure for these blends with dilatometry. The arrow in Figure 9 indicates the trend of the effect of deuteration on χ_{vol} and $\chi_{contact}$.

Phase Separation Morphology for PSD/PVME and PSH/PVME Blends by Optical Microscopy. Optical microscopy is a technique for studying the morphological features for both spinodal decomposition and nucleation and growth mechanisms of phase separation for polymer blends.[14] Figure 10 shows the time evolution for phase size growth for 30/70 wt % PSD/PVME at 170 °C and PSH/PVME at 130 °C. These temperatures correspond to equal degrees of superheating. The phases are interconnected during the initial stages of phase separation, during which the domains are constant in size. The phase domains then grow in size while maintaining their con-

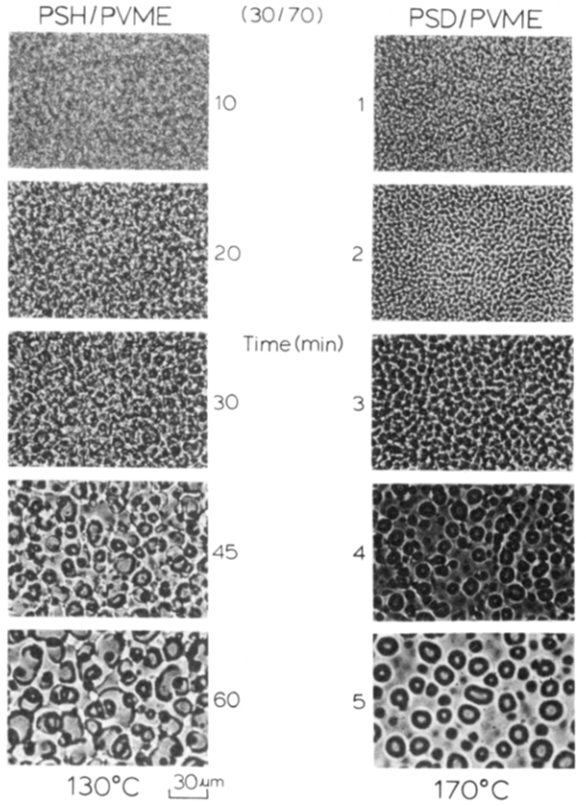

Figure 10. Optical micrograph of the time evolution of the phase separation behavior for the critical composition (30/70 wt %) of PSH/PVME and PSD/PVME at 130 °C and 170 °C, respectively.

Table III
a_T Value Calculated from the WLF Equation for 30/70 Wt % PSD/PVME and PSH/PVME Blends

blends	T, °C	$a_T \times 10^{14}$
PSD/PVME	168.0	2.58
PSD/PVME	170.0	2.61
PSH/PVME	127.0	17.08
PSH/PVME	130.0	14.08

nectivity, while in the latter stages the phases break into small spheres and then merge into macrospheres. These characteristics agree with the Cahn and Hilliard prediction for the early stages[27,28] and coarsening process for the late stages[29-33] of the spinodal decomposition and are similar to the morphological features observed by Nishi et al.[14] in the same blend with a different molecular weight. One finds a large difference in the kinetics of spinodal phase separation between PSD/PVME and PSH/PVME. It takes 10 times as long for the domains to grow for PSH/PVME as it does for PSD/PVME blends for these temperatures. This can be explained by the WLF equation,[34] which describes the temperature dependence of polymer diffusion

$$\log (a_T) = \log \left(\frac{\eta(T)}{\eta(T_g)} \right) = \frac{-C_1(T - T_g)}{C_2 + T - T_g} \qquad (4)$$

where η is the viscosity and C_1 and C_2 are constants. We have seen that T_g is approximately the same for PSH and PSD blends of the same composition. It is assumed that the phase growth is diffusion controlled. From the value of a_T calculated from eq 4 with $C_1 = -17.44$ and $C_2 = 51.6$ shown in Table III, it can be seen that the diffusion constant of PSD/PVME is greater than that of PSH/PVME blends by about a factor of 6. Thus phase growth will be faster for the PSD blends, since it will be at a temperature further above its T_g than will be the PSH blend at the same degree of superheating.

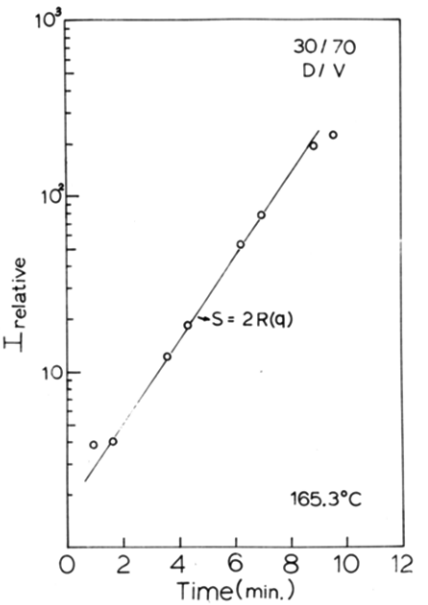

Figure 11. Plot of ln $[I(q,t)]$ vs. t for the early stage of spinodal decomposition of 30/70 PSD/PVME at 165.3 °C. The slope gives the growth rate $(2R(q))$.

Kinetics of Spinodal Decomposition for PSD/PVME and PSH/PVME Blends. Early Stages of Spinodal Decomposition. The light scattering data of the early stages of phase separation in the unstable region for polymer blends can be treated by the Cahn–Hilliard (C/H) linearization theory of spinodal decomposition[27,28] described elsewhere.[18,35] According to that theory, the change of elastic scattered intensity (I_{Vv}) with time (t) arising from the concentration fluctuation can be described by[36]

$$I_{Vv} = \tfrac{1}{4} (4\pi^2/\lambda^2)^2 I_0 V (\partial\alpha/\partial\phi)^2 [A^2(q) + B^2(q)] \exp[2R(q)t] \qquad (5)$$

or simply by

$$I_{Vv} \sim \exp[2R(q)t] \qquad (6)$$

where

$$R(q) = -Mq^2\{(\partial^2 G/\partial\phi^2) + 2\kappa q^2\} \qquad (7)$$

and ϕ is the volume fraction of one component of the mixture. The quantity α is the polarizability, assuming it is isotropic, $A(q)$ and $B(q)$ are the amplitudes of a given wave number q ($q = (4\pi/\lambda) \sin(\theta/2)$, where λ is the wavelength and θ is the scattering angle in the medium), $R(q)$ is the growth rate, M is the mobility constant of the molecules, and G is the free energy of the mixture.

$R(q)$ can be obtained from the slope of a plot of ln $I(q,t)$ vs. t shown in Figure 11 for 30/70 PSD/PVME. Then, the plot of $R(q)/q^2$ vs. q^2, shown in Figure 12, gives the "apparent diffusion coefficient (D_{app})", where $D_{app} = -M(\partial^2 G/\partial\phi^2)$, from eq 7. In the nucleation and growth regime, $\partial^2 G/\partial\phi^2$ is positive (the blend being stable to infinitesimal fluctuations), leading to a negative $R(q)$. In the spinodal decomposition regime, $\partial^2 G/\partial\phi^2$ is negative (the blend being unstable to the infinitesimal fluctuations), and hence $R(q)$ is positive for the value of q smaller than the critical q (q_c). Therefore, the spinodal point (T_s) can be obtained by extrapolating D_{app} to zero from a D_{app} vs. T plot[18] shown in Figure 12. The characteristic parameters for a 30/70 wt % blend of PSD/PVME and PSH/PVME are listed in Table IV. As previously discussed, the diffusion constant for PSD/PVME is about 6 times larger

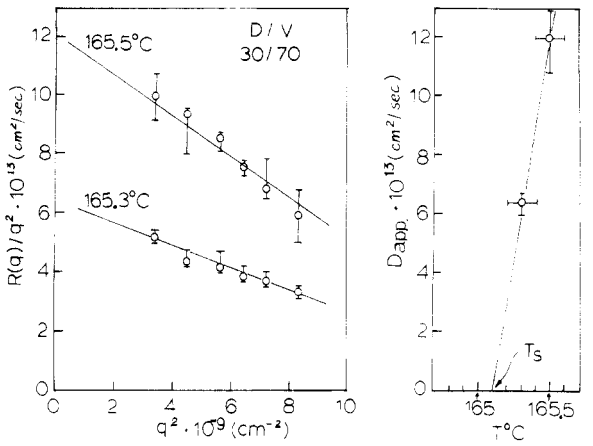

Figure 12. Data analysis in the linear spinodal decomposition for 30/70 PSD/PVME: (a) $R(q^2)/q^2$ vs. q^2 at different isothermal phase separation temperature, where $R(q)/q^2$ gives D_{app}; (b) temperature dependence of D_{app}, from which the spinodal temperature T_s = 165.1 °C is deduced.

Table IV
Characteristic Parameters Describing the Early Stage of Spinodal Decomposition of 30/70 PSD/PVME and PSH/PVME Blends

blend	$D_{app}/\Delta T$, cm²·s⁻¹·deg⁻¹	$q_m^2(t=0)/\Delta T$, cm⁻²·deg⁻¹
PSH/PVME	5.0×10^{-3}	1.54×10^{8}
PSD/PVME	30.0×10^{-13}	3.16×10^{8}

blend	T_s, °C	T_{exptl}	ΔT	D_{app}, cm²·s⁻¹	$q_m(t=0)$, cm⁻¹
PSH/PVME	124.2	127.0	2.8	1.4×10^{-12}	2.15×10^{5}
PSH/PVME	124.2	130.0	5.8	2.9×10^{-12}	3.04×10^{5}
PSD/PVME	165.1	168.0	2.9	8.7×10^{-12}	3.08×10^{5}
PSD/PVME	165.1	170.0	4.9	14.7×10^{-12}	3.97×10^{5}

than that of PSH/PVME, which explains the difference in kinetics of phase separation observed from optical microscopy. One can discuss this effect in a more quantitative way. According to Hashimoto et al.[18]

$$D_{app} \sim D_c(\partial \ln \chi/\partial T)_{T_s}\Delta T \tag{8}$$

and

$$q_m^2 \sim (1/R_0^2)(\partial \ln \chi/\partial T)_{T_s}\Delta T \tag{9}$$

where R_0 is the radius of gyration of the constituent polymers, D_c is the self-diffusivity, (each polymer was assumed to have identical D_c and R_0), and $\Delta T = T - T_s$, T_s being the spinodal temperature. Consequently, $D_{app}/\Delta T$ depends on $(\partial \ln \chi/\partial T)_{T_s}$ as well as on D_c as discussed above. The ratio D_{app}/q_m^2 is independent of $(\partial \ln \chi/\partial T)_{T_s}$ and depends primarily on D_c since R_0 hardly changes with temperature.

$$D_{app}/q_m^2 \sim D_c R_0^2 \sim D_c \tag{10}$$

The difference in $q_m^2/\Delta T$ between PSH/PVME and PSD/PVME is also of interest. From eq 9, the difference is primarily attributed to the difference in $(\partial \ln \chi/\partial T)_{T_s}$. It is well conceivable that the value $(\partial \ln \chi/\partial T)_{T_s}$ is different for the PSH and PSD blend systems because T_s is different and the temperature dependence of χ may also be different.

Late Stages of Spinodal Decomposition. The small-angle light scattering pattern obtained during the course of spinodal phase separation of PS/PVME blends shows a circular halo (Figure 2) due to spatial periodicity in concentration. The scattering angle of maximum intensity is shifted toward smaller angles (or smaller scattering vector) and the intensity increases with time, as

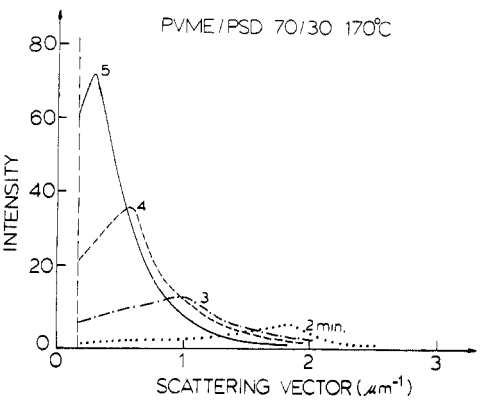

Figure 13. Scattered intensity (I) vs. scattering vector ($q = (4\pi/\lambda)\sin(\theta/2)$) for late stage of spinodal decomposition of 30/70 PSD/PVME at 170 °C.

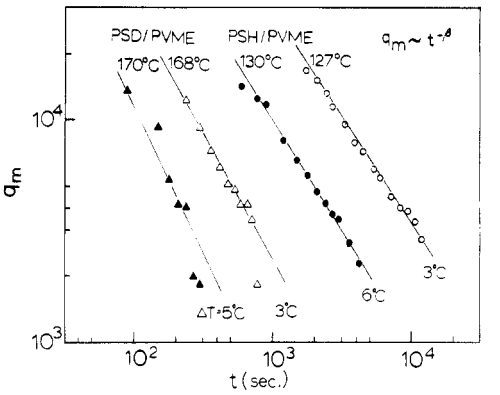

Figure 14. Maximum scattering vector (q_m) vs. time for 30/70 PSD/PVME and PSH/PVME blends.

shown in Figure 13 for 30/70 PSD/PVME at 170 °C. The maximum scattering vector magnitude (q_m) for both PSD/PVME and PSH/PVME as a function of time was fitted by a power-law expression proposed by Langer et al.[29] and Binder[30] et al.

$$q_m \sim t^{-\beta} \tag{11}$$

and plotted in Figure 14. Both systems show the same β, value which is close to 1. Further analysis of the time evolution of q_m may be necessary to determine the difference of phase separation kinetics due to deuterium substitution. The reduced-variable approach, which was used in the earlier works by Chou and Goldburg[37] and Langer et al.,[29] and later by Snyder,[38] can be applied to compare PSD/PVME with PSH/PVME blends. The reduced variables, time, and wavenumber (which are dimensionless quantities) can be defined by

$$\tau = \frac{t}{(\xi^2/D_{app})} \tag{12}$$

$$Q_m(t) = q_m(t)\xi \tag{13}$$

where ξ is the correlation length at the quench time and can be obtained by

$$\xi = 1/q_m(t=0) \tag{14}$$

The master curve of reduced wavenumber (Q_m) vs. reduced time (τ) for PSD/PVME and PSH/PVME is plotted in Figure 15, and gives an exponent 1.0 according to eq 11 (in this case, $Q_m \sim \tau^{-\beta}$), which is in good agreement with Snyder's data[40] on PSH/PVME blends during late stages of phase separation. Snyder also used this approach to compare other systems such as metallic alloys, inorganic glasses, and small-molecule systems and concluded that

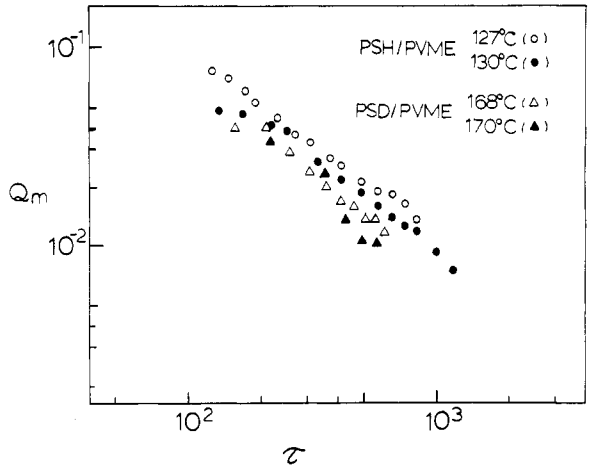

Figure 15. Reduced wavenumber (Q_m) vs. reduced time (τ) plot for PSD/PVME and PSH/PVME blends at various temperatures.

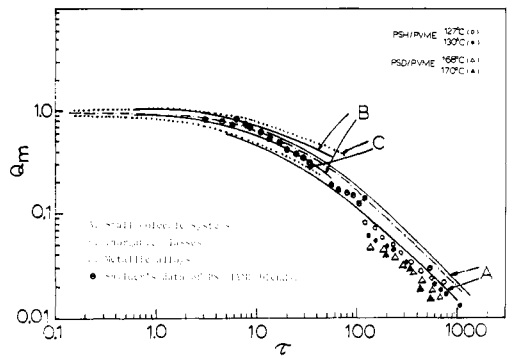

Figure 16. Master curve for the phase separation process of PSD/PVME and PSH/PVME blends compared to other systems.

the phase separation in all cases was governed by similar dynamics. Our work on PSD/PVME and PSH/PVME is also compared to other systems and Snyder's data of PSH/PVME blends with different quench depth and molecular weight in Figure 16. It can be seen that all the data fall on the same master curve. Experimentally, there is no consistency to the reported power laws. For example, values of β have been reported varying from $\beta = 0$ to $\beta = 1$. It is believed that the observed power relation depends strongly on the system being studied, the composition of the mixture, and the quench depth. Recently, Nose et al.[39] and Hashimoto et al.[40] have shown a composition dependence of the exponent. They found that at the critical composition β is 1 and it may be around $^1/_3$ in other conditions. Considering the composition studied and the observations on the extent to which phase separation has occured, our experimental results are consistent with the both data of Snyder et al. and Hashimoto et al. Consequently, there are no specific differences in the phase separation mechanism due to deuterium substitution in the blends, and differences in the rate of growth, $R(q)$, of PSD/PVME and PSH/PVME are due to differences in diffusion behavior arising from the difference between the LCST and T_g for the two cases.

Conclusions

The substitution of deutereous polystyrene (PSD) for hydrogenous polystyrene (PSH) in PS/PVME blends raised the LCST of the blend by about 40 °C. This deuteration effect should be considered in measuring the interaction parameter of quasi-ternary systems (e.g., PSD/PSH/PVME) by means of the SANS technique. The effect has been qualitatively related to the larger percentage of negative volume of mixing for PSD/PVME relative to that for PSH/PVME, where the contribution of $\chi_{contact}$ due to deuteration outweighs χ_{vol} and results in an increase in the LCST for this blend. If the P–V–T data of the blends can be measured, then the deuteration effect may be interpreted more quantitatively by using the equation-of-state approach. Furthermore, one should measure the χ_{HS} and χ_{DS} by measuring the scattering intensity of the H/S and D/S blends separately. D/S blends can be conveniently investigated with SANS,[8,41] but H/S blends will be difficult to study because of the poor scattering contrast.

Using fluorescence emission methods, Monnerie et al.[16] have also observed a similar deuteration effect for the case of PS/PVME blends. They also studied systems[42] where PS was specifically deuterated, i.e., on the benzene ring or on the main chain. They found that the cloud points for PS with deuteration of the ring were similar to those for PSD/PVME systems and cloud points for PS with main-chain deuteration were similar to those for the PSH/PVME systems. This finding indicates the possibility of some kind of interaction between the ring of PS and PVME. It is highly likely that the benzene ring of PS forms a complex with ether's lone pair of electrons of PVME. This kind of complex interaction has been suggested by Hsu et al.[43] and Garcia[44] based on the results of Fourier-transform infrared measurements. Therefore, replacement of PSH by PSD in PS/PVME blends changes the strength of the interaction between the two components. Recently, Koningsveld et al.[45] have also found the deuteration effect on the UCST behavior of PS/polybutadiene (PB) blends. It is shown that the spinodal curve of PS/PB blends is shifted by 14 °C toward higher temperature if the hydrogen in PB (PBH) is replaced by deuterium (PBD). By using the Flory–Huggins-type equation, assuming the interaction parameter is concentration dependent, they concluded that both the entropy and enthalpy of mixing are different between PS/PBD and PS/PBH. Apparently, any constituent in polymer blends that is deuterated for both LCST and UCST can shift the phase diagram to a higher temperature. It is noted that the blends with LCST behavior become more miscible, but those with UCST become more immiscible. It would be of interest to investigate the phase separation behavior when both components are deuterated in the blend.

As the result of DSC measurements, PSD/PVME and PSH/PVME have shown the same T_g value for the same composition. Optical microscopy has been applied to observe the morphology of phase separation of the blends, and their features are consistent with theoretical predictions. It turns out that the phase separation kinetics of PSD/PVME is about 10 times faster than that of the PSH/PVME blend at the same degree of superheating. This difference is qualitatively predicted by their viscosity value calculated from the WLF equation and the diffusion constant measured from the light scattering technique based on Cahn–Hilliard linearization theory. The lower viscosity and higher diffusion constant are found to account for the faster phase separation of PSD/PVME blends.

Furthermore, the dynamic parameters q_m and t of phase separation for PSD/PVME and PSH/PVME blends are scaled to the reduced variables Q_m and τ, respectively, in terms of the characteristic parameters D_{app} and $q_m(t=0)$. Both blends are found to have phase separation processes similar to those of other systems such as metallic alloys, inorganic glasses, and small-molecule systems. Their exponent has the same value (1.0) according to the power-law approach, consistent with the data of Hashimoto et al.[40]

at the critical composition. Therefore, the phase separation kinetics for PSD/PVME is much faster than that for PSH/PVME with the same degree of superheating simply due to its lower viscosity and higher diffusion constant.

Acknowledgment. We gratefully acknowledge financial support from the National Science Foundation, the Materials Research Laboratory of the University of Massachusetts, and Japan Society for Promotion of Science. We also thank Dr. R. Koningsveld for his helpful discussion and comments.

Registry No. PS, 9003-53-6; PVME, 9003-09-2.

References and Notes

(1) Kirste, R. G.; Kruse, W. A.; Ibel, K. *Polymer* **1975**, *16*, 20.
(2) Schmitt, B. J.; Kirste, R. G.; Jelenic, J. *Makromol. Chem.* **1980**, *181*, 1655.
(3) Walsh, D. J.; Higgins, J. S.; Doube, C. P.; Mckeown, J. G. *Polymer* **1981**, *22*, 168.
(4) Wignall, G. D.; Child, H. R.; Li-Aravena, F. *Polymer* **1980**, *21*, 131.
(5) Ballard, D. G. H.; Rayner, M. G.; Schelten, J. *Polymer* **1976**, *17*, 640.
(6) Russell, T. P.; Stein, R. S. *J. Polym. Sci., Polym. Phys. Ed.* **1982**, *20*, 1593.
(7) Warner, M.; Higgins, J. S.; Carter, A. J. *Macromolecules* **1983**, *16*, 1931.
(8) Jelenic, J.; Kirste, R. G.; Oberthur, R. C.; Schmitt-Strecher, S.; Schmitt, B. J. *Makromol. Chem.* **1984**, *185*, 129.
(9) Hadziioannou, G.; Stein, R. S. *Macromolecules* **1984**, *17*, 567.
(10) Maconnachie, A.; Kambour, R. P.; Bopp, R. C. *Polymer* **1984**, *25*, 357.
(11) Cotton, J. P.; Decker, D.; Benoit, H.; Farnoux, B.; Higgins, J.; Jannix, G.; Ober, R.; Picot, C.; des Cloizeaux, J. *Macromolecules* **1974**, *7*, 863.
(12) Strazielle, C.; Benoit, H. *Macromolecules* **1975**, *8*, 203.
(13) Bank, M.; Leffingwell, J.; Thies, C. *J. Polym. Sci., Part A-2* **1972**, *10*, 1097.
(14) Nishi, T.; Kwei, T. K. *Macromolecules* **1975**, *8*, 227.
(15) Yang, H.; Hadziioannou, G.; Stein, R. S. *J. Polym. Sci., Polym. Phys. Ed.* **1983**, *21*, 159.
(16) Halary, J. L.; Ubrich, J. M.; Monnerie, L.; Yang, H.; Stein, R. S. *Polym. Commun.* **1985**, *26*, 73.
(17) Reich, S.; Cohen, Y. *J. Polym. Sci., Polym. Phys. Ed.* **1981**, *19*, 1255.
(18) Hashimoto, T.; Kumaki, J.; Kawai, H. *Macromolecules* **1983**, *16*, 641.
(19) Tabar, R. J.; Long, M. B.; Stein, R. S. *J. Polym. Sci., Polym. Phys. Ed.* **1982**, *20*, 2041.
(20) McMaster, L. P. *Macromolecules* **1973**, *6*, 760.
(21) Bank, M.; Leffingwell, J.; Thies, C. *Macromolecules* **1971**, *4*, 43.
(22) Shur, Y. J.; Randy, B. *J. Appl. Polym. Sci.* **1975**, *19*, 1337, 2143.
(23) Work, J. L. *Polym. Eng. Sci.* **1973**, *13*, 46.
(24) Hickman, J. J.; Ikeda, R. M. *J. Polym. Sci., Polym. Phys. Ed.* **1973**, *11*, 1713.
(25) Zakrzewski, G. A. *Polymer* **1973**, *14*, 347.
(26) Kwei, T. K.; Nishi, T.; Roberts, R. F. *Macromolecules* **1974**, *7*, 667.
(27) Cahn, J. W. *J. Chem. Phys.* **1965**, *42*, 93.
(28) Cahn, J. W. *Trans. Met. Soc. AIME* **1968**, *242*, 166.
(29) Langer, J. S.; Bar-on, M.; Miller, H. S. *Phys. Rev. A* **1975**, *11*, 1417.
(30) Binder, K.; Stauffer, D. *Phys. Rev. Lett.* **1974**, *33*, 1006.
(31) Kawasaki, K.; Ohta, T. *Prog. Theor. Phys.* **1978**, *59*, 362.
(32) Lifshitz, I. M.; Slyozov, V. V. *J. Phys. Chem. Solids* **1961**, *19*, 35.
(33) Siggia, E. D. *Phys. Rev. A* **1979**, *20*, 595.
(34) Williams, M. L.; Landel, R. F.; Ferry, J. D. *J. Am. Chem. Soc.* **1955**, *77*, 3701.
(35) Snyder, H. L.; Meakin, P.; Reich, S. *Macromolecules* **1983**, *16*, 757.
(36) van Aartsen, J. J.; Smolders, C. A. *Eur. Polym. J.* **1970**, *6*, 1105.
(37) Chou, Y. C.; Goldburg, W. I. *Phys. Rev. A* **1979**, *20*, 2105.
(38) Snyder, H. L.; Meakin, P. *J. Chem. Phys.* **1983**, *79*(11), 5588.
(39) Nojima, S.; Ohyama, Y.; Yamaguchi, M.; Nose, T. *Polym. J.* **1982**, *14*, 907.
(40) Shimizu, N.; Itakura, M.; Hashimoto, T. *Macromolecules*, submitted.
(41) Shibayama, M.; Yang, H.; Stein, R. S.; Han, C. C. *Macromolecules* **1985**, *18*, 2179.
(42) Ben Cheiki Larbi, F.; Leloup, S.; Halary, J. L.; Monnerie, L. *Polym. Commun.* **1986**, *27*, 23.
(43) Lu, F. J.; Benedetti, E.; Hsu, S. L. *Macromolecules* **1983**, *16*, 1525.
(44) Garcia, D. *J. Polym. Sci., Polym. Phys. Ed.* **1984**, *22*, 107.
(45) Atkin, E. L.; Kleintjen, L. A.; Koningsveld, R.; Fetters, L. J. *Polym. Bull. (Berlin)* **1982**, *8*, 347; *Makromol. Chem.* **1984**, *185*, 377.

Charge-Transfer Complexes between Molecular Oxygen and Polystyrenes

J. F. Rabek,* J. Sanetra,† and B. Rånby

Department of Polymer Technology, The Royal Institute of Technology, S-10044 Stockholm, Sweden. *Received October 9, 1985*

ABSTRACT: Contact charge-transfer complexes (CTC complexes) between polystyrene, poly(α-methylstyrene), poly(*p*-methylstyrene), poly(*p*-isopropylstyrene), poly(*p*-chlorostyrene), poly(*p*-bromostyrene), and molecular oxygen have been investigated at different oxygen pressures by absorption spectroscopy. At high oxygen pressures formation of CTC complexes increases, whereas intensity of excimer emission decreases. These phenomena are reversible and reproducible. The poly(*p*-methoxystyrene) does not form a CTC complex with oxygen because of the sterical effect. The main feature of these CTC complexes is the extension of the absorption range of polystyrenes in the presence of oxygen. Formation of CTC complexes may have an important role in the increased absorption of light by polystyrenes and participate in the initiation step of photodegradation.

Introduction

The formation of a charge-transfer complex (CTC complex) between molecular oxygen and organic compounds such as alcohols,[1,2] ethers,[1,3] amines,[2,4] and aromatic hydrocarbons[2,4-6] was reported more than 20 years ago. Styrene forms a CTC oxygen complex, which then participates in the photopolymerization of this monomer.[7,8] The rate of photopolymerization of ethylene is accelerated in the presence of oxygen.[9] This fact has been attributed to the formation of a CTC complex and to an enhanced singlet–triplet transition of ethylene induced by magnetic perturbation due to oxygen.

Formation of CTC complexes has also been proposed for polyolefins[10] and polystyrene.[11-13] More detailed knowledge on the formation of the CTC complexes could

* To whom all correspondence should be addressed.
† Present address: Department of Physics, Technical University, Krakow, Poland.

0024-9297/86/2219-1674$01.50/0